#5485

SOIL GAS AND RADON ENTRY POTENTIALS FOR SLAB-ON-GRADE HOUSES

by: Bradley H. Turk
105 E. Marcy St., Rm. 109
Santa Fe, NM 87501

David Grumm, Yanxia Li, and Stephen D. Schery
Physics Department
New Mexico Institute of Mining and Technology
Socorro, NM 87801

D. Bruce Henschel
AEERL
U.S. EPA
Research Triangle Park, NC 27711

ABSTRACT

The technique to quantify the potential for pressure-driven entry of soil gas and radon through house surfaces in contact with the soil is evaluated for six New Mexico houses with slab-on-grade floors. Flows, pressures, and radon concentrations were measured through test holes in these floors while the houses were mechanically depressurized from -10 to -30 Pa. Soil and substructure surface resistances, and soil gas and radon entry potentials were calculated for each test location. These data support earlier work in four basement houses in New Jersey that showed the soils surrounding a building's substructure are many times more resistant to soil gas movement than the substructure surfaces themselves. Locations along the perimeter of the slab floors had soil gas entry potentials approximately 40 times greater and radon entry potentials approximately 15 times greater than locations more central to the slab. Mean radon entry potentials for a house were found to be a satisfactory indicator of the average indoor radon concentrations during the heating season. The radon entry potential data were also useful in the design and placement of subsurface depressurization radon mitigation systems in these houses where system locations that are acceptable to the homeowners are limited.

OVERVIEW

For both scientific and practical reasons, it is important to be able to characterize the convective flow of soil gas and radon through the surrounding

soils, materials, and constructed surfaces of individual buildings. Information on this movement can improve our understanding of the basic physical mechanisms at work in and around actual buildings. It can also provide guidance on the selection and design of techniques to reduce radon levels inside buildings where elevated concentrations may pose an excessive health risk.

A technique developed two years ago by one of the authors (1) quantifies the relative leakiness of substructure surfaces in contact with the soil and the resistance to soil gas movement of the soils and materials around a building. The technique also has proven useful in guiding the placement of subsurface depressurization (SSD) radon control systems. The objective of the technique is to develop entry potentials for soil gas and radon at various locations in the substructure surfaces assuming that the detailed characteristics of the substructure surfaces and surrounding soils cannot be known. Interpretive and measurement methods are based on the procedures of researchers investigating the radon source potential of soil (2,3,4) and the pressure fields created in the soil around houses (5,6). Entry potentials were originally evaluated in four New Jersey (NJ) houses with basements. In this paper, the technique is examined in six slab-on-grade houses in New Mexico (NM).

DEFINING SOIL GAS AND RADON ENTRY POTENTIALS

For many existing buildings it is impossible to know the specific details of the usually complex and non-uniform structure construction and underlying soils and materials. Consequently, a complete understanding of soil gas and radon movement around and into a building is unattainable. Similar to the work of others (7,8), a steady-state lumped parameter model seeks to simplify the building/soil system by substituting a few simple electrical circuit elements for the many detailed structure and soil features. We assume that at each soil gas/radon entry location the building 'views' an aggregation of the network of pathways through the local cracks, gaps, and low and high permeability regions in the below-grade soils, materials, and construction features around the substructure. Likewise, the entry location itself is affected by nearby imperfections in the substructure surfaces. If air flow through all of these materials is laminar, a direct current electrical analog may be applied where air flow is represented by electrical current and pressure differences by voltage drops. At each test location we create a series circuit by substituting an effective resistor for the complex network of resistances in the surrounding soil and another resistor for the substructure surface. The negative pressure found in the building is substituted by a battery (see Figure 1). Other researchers have developed lumped parameter models to more accurately represent the transient conditions of an actual building (9). The circuits in these models include capacitors -- which would involve longer-term, more complex experimental procedures.

To determine the values of the circuit parameters, a test hole is drilled through a substructure surface. While the negative pressure in the building is mechanically enhanced by a blower, the pressure difference (ΔP, "voltage drop") across the sealed test hole is measured. The measured ΔP depends on the resistance of the substructure surface relative to the resis-

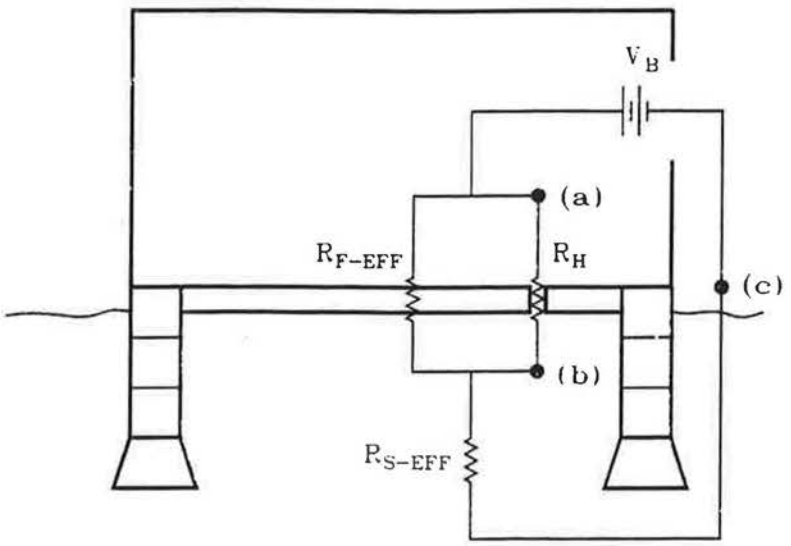

Figure 1. A simplified electrical circuit is shown that substitutes for the resistances to soil gas flow through the soil and substructure materials.

tance of the surrounding soils. A ratio of these two resistances, Z, is defined as

$$Z = \frac{P_{HC}}{P_{SC}} = \frac{V_{HC}}{V_{SC}} = \frac{I_{TC}R_{FC-EFF}}{I_{TC}R_{SC-EFF}} = \frac{R_{FC-EFF}}{R_{SC-EFF}}, \qquad [1]$$

where (a subscript "C" identifies the condition with the test hole closed):

P_B (V_B) = measured pressure difference (or "applied voltage") between inside of house/substructure and outdoors, point a to c (Pa).

P_H (V_H) = measured pressure (or "voltage") drop across open test hole and flow adaptor, point a to b (Pa).

P_S (V_S) = calculated pressure drop across soil paths between point b and outdoors (c) with test hole open, P_B - P_H (Pa).

Q_T (I_T) = defined total flow ("current") through cracks, openings, and test hole (m^3/s).

R_{F-EFF} = calculated effective resistance that lumps resistances of cracks and openings in substructure surfaces and resistances of near-substructure materials surrounding the open test hole ($Pa-s/m^3$). and

R_{S-EFF} = calculated effective resistance of soil paths to measurement point b with test hole open ($Pa-s/m^3$).

Typically, a low resistance (leaky) surface will cause a smaller ΔP to be measured across the sealed test hole. To determine the effective resistance of the surrounding soils, the air flow through open test holes is measured. Because the test hole is not a perfect short circuit -- soil gas continues to

pass through nearby cracks and openings in the substructure surface -- the ΔP across the test hole is measured with the test hole open. Assuming that $R_{FC-EFF} \approx R_{F-EFF}$ and $R_{SC-EFF} \approx R_{S-EFF}$, then performing circuit analysis and substituting analogous air flow and pressure parameters, the effective soil resistance is calculated from

$$R_{S-EFF} = \frac{P_B - P_H\left(1 + \frac{1}{Z}\right)}{Q_H}. \qquad [2]$$

where Q_H (I_H) = measured (corrected) flow through open test hole and flow adaptor (m^3/s). The effective resistance of the substructure surface, R_{F-EFF}, is found from Equation [1].

The entry potential of soil gas at a test location, G ($m^3/Pa\text{-}s$), is proportional to the soil gas flow through surrounding soil and materials and nearby cracks and openings in the substructure surface. It is defined as a net conductance:

$$G = \frac{1}{R_{S-EFF} + R_{F-EFF}}. \qquad [3]$$

The radon entry potential, E ($Bq/Pa\text{-}s$), is defined as the mass transfer of radon in the soil gas near the substructure surface, C (Bq/m^3), with the pressure-normalized flow of soil gas into the building:

$$E = GC. \qquad [4]$$

Thus, if soil and subsurface effective resistances are low, the potential for soil gas to enter a building is increased. In addition, if radon levels in the soil gas are elevated, then the potential for radon to enter a building through an area near a test hole is also increased. The term 'potential', used to define soil gas and radon movement into buildings, does not refer to electrical potential. Instead it is a more casual term for the possibility, or capability, of soil gas or radon to enter near a particular test location.

DESCRIPTION OF HOUSES AND EXPERIMENTAL PROCEDURES

The six New Mexico houses that were studied for this paper are located in or around Santa Fe and Albuquerque. They are part of an eight-house research project in New Mexico investigating radon and thoron entry and control. All six houses are single story and have slab-on-grade construction. Typically, the slab floors were poured over compacted existing soil, although fill material containing some gravel was used in part of one house (AL04). Existing soils range from slightly expansive clays to coarse sandy loam with rock fragments. Where the slabs are exposed, hairline cracks are often visible, although most slabs are covered with carpet, linoleum, or tile. At least one house (TI42) appears to have a monolithic (downturn) slab, while the remaining houses have floating slabs inside of concrete block or poured concrete stem walls. In every house but AL04, extensive cracks (up to 10 mm wide) exist along the perimeter at the slab/stem wall boundary. These cracks are sometimes aggravated by styrofoam insulation panels placed vertically on

the inside of the stem wall. Horizontal sheets of styrofoam insulation were found directly below the slab along the perimeter walls in other houses. Plumbing services are always routed below the floor, as well as forced air furnace supply ducts in some houses (AL02, AL03, and AL04).

EXPERIMENTAL PROCEDURES

From five to thirteen 16 mm (5/8 in.) diameter holes were drilled through the slab at accessible locations in each house. The holes were placed to be accessible to the researchers, to avoid sub-floor services, and to satisfy the aesthetic requirements of the homeowners. By comparison, approximately 30 test holes were drilled through the surfaces of unoccupied substructures in each New Jersey house. A blower door fan was used to mechanically depressurize the houses to approximately -10 Pa and -30 Pa. At each test hole radon grab samples of soil gas were collected first and then air flows and ΔPs were measured during depressurization. The enhanced depressurization minimized environmental influences and increased the magnitude of the flow and ΔP so they could be more easily measured.

Radon grab samples were collected through a filtered sample train into evacuated 300 cm^3 alpha scintillation flasks. Alpha activity in the cells was counted after a 3-hour delay on a portable counter/scaler (Pylon Model AB-5). Uncertainties with this technique are estimated to be ±20%.

Pressure differences were measured using an electronic micromanometer (Neotronics Model MP20SR) with a minimum resolvable ΔP of 0.1 Pa with a specified accuracy of 1% of full scale. All ΔPs were measured with the house as reference. Pressure differences were first measured across the slab at each test hole with all holes sealed, P_{HC}. Then the ΔP was measured across the open hole with a flow adaptor in place, P_H. An alternative approach would be to calculate the ΔP across the open test hole using a standard engineering formula. The flow adaptor is used to establish uniform flow and pressure measurement conditions at each test hole and is slightly modified from the adaptor used in the New Jersey houses (1). The adaptor is a 0.3 m (12 in.) long metal tube with an inside diameter of approximately 10 mm (the outside diameter is 1/2 in.). A small diameter (3 mm, 1/8 in.) static pressure tube runs along the inside length of the adaptor to sense pressure at the end placed into the test hole. A fitting into the side of the adaptor allows a hot wire anemometer probe to be inserted into the air stream within the adaptor. Flow rates less than 0.015 m/s (3 fpm) could not be reliably measured on the Hastings Model B-22 hot wire anemometer. Calculated flow through the adaptor could be in error by as much as ±50%.

RESULTS

Data from this study of New Mexico houses are shown in Tables 1, 3, and 4 and in Figures 2, 3, and 4. Effective resistances and entry potentials were calculated using Equations [1] through [4]. Where measured flows and pressures were less than the detection limits of the instrumentation, values of

approximately half the detection limit were substituted into the calculations.

The summary in Table 1 includes statistics for both normal and lognormal distributions. However, since cumulative probability plots of the data indicate that the data are most closely approximated by the lognormal distribution, subsequent tables only present the geometric mean (GM) and geometric standard deviation (GSD). Aggregation of the test locations under one statistical grouping (as in the first grouping of Table 1) can be misleading. These summary statistics for all test locations at all houses or for one house alone are not a true average representation since the test holes were not randomly located or spaced to include the entire floor area.

In Table 2, data are presented from the earlier New Jersey study. Since the method of flow measurement was slightly different and the ΔP at the test hole, P_H, was calculated rather than measured, the data may not be exactly comparable to those in this study.

DISCUSSION

SUBSTRUCTURE, REGIONAL, AND TEST LOCATION COMPARISONS

Table 1 summarizes the entry potential parameters from the -10 Pa depressurization test at the 48 NM test locations. The GSD for all data is large indicating a very large range in the value of the parameters. By examining the GM for the soil and surface effective resistances, it is apparent that the soil surrounding the houses is from 5 to 13 times more resistant to soil gas flow than slab floor surfaces. This is consistent with the earlier data in the NJ houses (Table 2) which show that soils were between two and six times more resistant to soil gas flow than the substructure surfaces. The GM soil gas entry potentials for the NM slab-on-grade floors tend to be higher than for the NJ basement floors, possibly due to more permeable soils surrounding the NJ houses (although data on soil permeability are not yet available) or to the closer proximity to the outdoor soil grade in the NM houses. The NM data have been grouped according to location of the test hole: a) within 1 m of the slab perimeter, and b) interior locations farther than 1 m from the slab perimeter. The perimeter locations have much higher soil gas entry potentials (and lower soil and surface resistances). Proximity to outdoor soil grade, the extensive cracking observed along the perimeter, and the disturbed soil and materials around the stem walls and footings probably combine to contribute to the very high soil gas entry potentials at these perimeter locations. Likewise, the soil gas entry potential for block wall cavity locations in the NJ houses is slightly higher -- also possibly due to the same factors affecting the perimeter locations in the NM slabs-on-grade. The interior locations in the NM houses generally had poor pressure field connection to other locations as measured with SSD mitigation systems operating or with the sub-slab vacuum cleaner test.

For both NM and NJ houses, where soil gas entry potentials are low, the radon concentrations in the soil gas tend to be high. The low soil gas entry potentials may be indicative of poor flushing of radon from the soil by slight

soil gas movement into the buildings and by minimal diffusion over the large distance to the soil surface. The GM soil gas radon concentrations were higher for the NJ houses than the NM houses, suggesting a larger radon source in the NJ soils. These higher soil gas radon concentrations (42000 Bq/m^3) resulted in the NJ houses' having a high GM radon entry potential through the basement floors. However, the relatively high soil gas entry potential for perimeter slab locations in the NM houses created a high radon entry potential (GM of 15 $\times$ 10^{-3} Bq/Pa-s) despite the low GM radon concentration of 3000 Bq/m^3. The GM radon entry potential for interior slab locations in the NM houses was 15 times lower than for the perimeter locations, despite the higher GM radon concentrations at the interior locations.

Table 1. Summary of Entry Potential Parameters at -10 Pa Calculated for New Mexico Slab-on-Grade Houses

Statistic	Entry Potential Parameters				
	Soil Resistance, R_{S-EFF} (10^6 Pa-s/m^3)	Surface Resistance, R_{F-EFF} (10^6 Pa-s/m^3)	Soil Gas Entry Potential, G (10^{-6} m^3/Pa-s)	Radon Conc. (kBq/m^3)	Radon Entry Potential, E (10^{-3} Bq/Pa-s)
All Locations at 6 Houses					
Geometric Mean	0.32	0.064	2.2	3.6	8.5
Geometric Std. Dev.	15.1	10.5	13.0	4.00	13.4
Arithmetic Mean	5.1	1.1	13	7.7	65
Arithmetic Std. Dev.	8.75	3.02	21.5	9.00	136
Number of Locations	48	48	48	47	47
Slab Perimeter Locations at 5 Houses					
Geometric Mean	0.20	0.038	4.6	3.0	15
Geometric Std. Dev.	10.9	7.73	9.22	4.09	11.0
Number of Locations	38	38	38	37	37
Interior Locations > 1 Meter from Perimeter at 5 Houses					
Geometric Mean	6.2	0.47	0.14	7.4	1.0
Geometric Std. Dev	6.18	12.1	6.16	2.92	9.58
Number of Locations	10	10	10	10	10

Table 2. Summary of Entry Potential Parameters Calculated for Four New Jersey Houses

Statistic	R_{S-EFF} (10^6 Pa-s/m^3)	R_{F-EFF} (10^6 Pa-s/m^3)	G (10^{-6} m^3/Pa-s)	Rn Conc. (kBq/m^3)	E (10^{-3} Bq/Pa-s)
Basement Slab Floor Locations					
Geometric Mean	1.2	0.65	0.5	42	23
Geometric Std. Dev.	5.0	4.8	4.8	8.09	6.7
Number of Locations	22	22	22	22	22
Basement Block Wall Cavity Locations					
Geometric Mean	0.68	0.12	1.2	6.5	7.9
Geometric Std. Dev	2.2	2.1	1.6	4.85	5.1
Number of Locations	44	44	44	42	42

RADON ENTRY POTENTIALS AND INDOOR RADON LEVELS

It is expected that houses with higher average radon entry potentials would have higher indoor radon levels. Figure 2 relates these data for the four NJ and six NM houses. The plot on the right of Figure 2 shows the modest correlation of the average indoor radon concentration during the winter with the GM radon entry potential for each group of houses. The two groups do not appear on the same line because of differences in house construction, number and location of the test holes at each house, and possibly measurement and averaging techniques. The left plot in Figure 2 displays the same data but normalized for each group by the median average radon concentration and median GM radon entry potential. The correlation coefficient, R, for these normalized data is 0.67. The data indicate that, with improved techniques, radon entry potentials may be a practicable predictor of long-term winter radon concentrations in some houses. In models of indoor air pollution, the indoor concentration of pollutants is not solely dependent on the pollutant source strength. Ventilation rates are also an important factor and may explain some of the lack of correlation in these data.

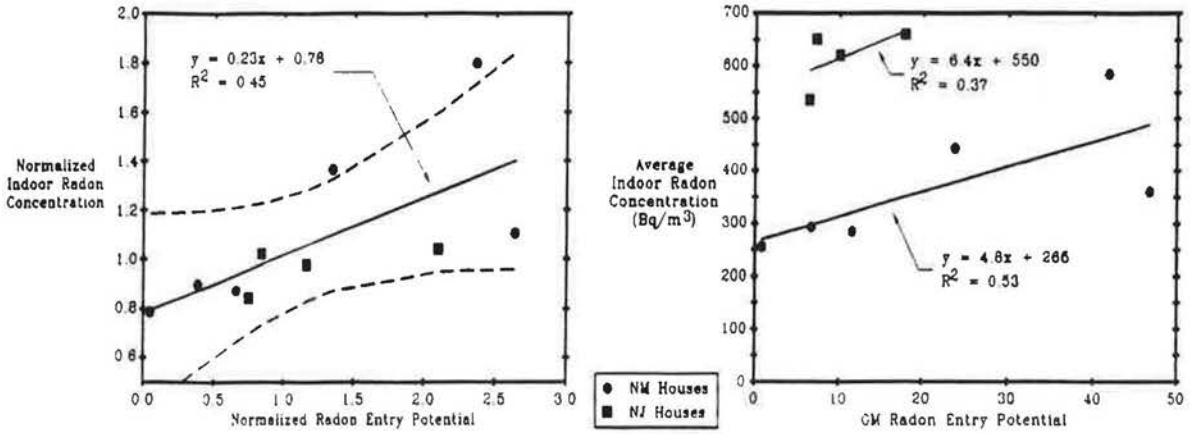

Figure 2. Average winter indoor radon levels for four NJ houses and six New Mexico houses are related to the GM radon entry potential at each house in the right plot. In the left plot, the data are normalized by the median for each group. Solid curves are lines of best-fit from linear regression. Dashed lines are 95% confidence curves.

ENTRY POTENTIALS AT DIFFERENT APPLIED DEPRESSURIZATIONS

At five of the six New Mexico houses, entry potentials were determined with the structure depressurized to both -10 and -30 Pa. The results at these two levels of depressurization are compared in Table 3. The same radon grab samples were used to calculate radon entry potentials for both pressures; however, flows and ΔPs changed, causing changes in the radon entry potential. A one-sided, two-sample, non-parametric test does not conclusively show that the soil gas entry potentials at -10 Pa are significantly higher than at -30 Pa ($p < 0.6$). The data from a similar comparison of applied pressures at 31 test locations in the NJ houses also indicate that there is little significant statistical difference ($p < 0.3$) in the soil gas entry potential for the

different pressures. However, because the range of values is large for these parameters (large GSD), the statistical tests are not conclusive. In addition, since the soil gas entry potential at -10 Pa is higher for 20 of the 26 test locations and for the GM of the group, there may be some bias in the procedure to cause this difference. The GM soil gas entry potential at approximately -10 Pa for the NJ test locations was 0.64×10^{-6} m³/Pa-s (GSD of 4.16) and at approximately -30 Pa was 0.47×10^{-6} m³/Pa-s. An analysis of flow data from 22 test holes in the NJ houses suggests that flow through those holes did not increase in direct proportion to the applied pressure. For a general equation of the form, $Q = A(\Delta P)^n$, the exponent, n, was calculated to be approximately 0.9. This result may be due to non-linear air flow through the materials below the test hole or within the flow adaptor, and could explain slightly lower entry potentials at higher pressures.

Table 3. Comparing Entry Potential Parameters at -10 and -30 Pa from 5 New Mexico Houses

Statistic	R_{S-EFF} (10^6 Pa-s/m³)	R_{F-EFF} (10^6 Pa-s/m³)	G (10^{-6} m³/Pa-s)	E (10^{-3} Bq/Pa-s)
House Depressurized to Approx. -30 Pa				
Geometric Mean	0.44	0.13	1.4	6.0
Geometric Std. Dev.	13.2			
House Depressurized to Approx. -10 Pa				
Geometric Mean	0.35	0.10	1.9	7.8
Geometric Std. Dev.	14.4	15.2	12.9	14.0
Number of Locations	26	26	26	26

SEASONAL CHANGES

Thus far in the study, entry potential measurements have been conducted in different seasons in only one house, AL03. The data for the measurements made at seven test locations in September and January are shown in Table 4. By inspection, it appears that the entry potentials are very similar for the two periods, although because of the small sample size and large standard deviation, the equality of the samples is not statistically robust ($p < 0.70$). It is conceivable that seasonal changes in environmental and structural conditions, and soil moisture could have a significant effect on the flows, pressures, and radon concentrations measured during an entry potential test. These additional measurements are planned for the remaining five houses.

Table 4. Comparison of Entry Potential Parameters for Two Seasons at New Mexico House AL03

Statistic	R_{S-EFF} (10^6 Pa-s.m³)	R_{F-EFF} (10^6 Pa-s/m³)	G (10^{-6} m³/Pa-s)	Rn Conc. (kBq/m³)	E (10^{-3} Bq/Pa-s)
September 1990					
Geometric Mean	[illegible]	2.0	0.12	4.2	0.50
Geometric Std. Dev.	[illegible]	3.92	7.36	2.15	8.14
January 1991					
Geometric Mean	[illegible]	1.5	0.12	4.5	0.34
Geometric Std. Dev.	[illegible]	4.68	8.01	3.00	6.05
Number of Locations	[illegible]	[illegible]	[illegible]	[illegible]	[illegible]

APPLYING ENTRY POTENTIALS TO SSD DESIGN

An important aspect of this work has been to apply the radon entry potential data to the design of SSD radon control systems. The material below the slabs in the center of these houses does not support the broad extension of a pressure field from an SSD pipe. Therefore, many pipes would have been required to develop an adequate pressure field beneath the entire slab. Since almost the total occupied floor area of these houses is finished, finding acceptable locations for SSD pipes is difficult.

Figures 3 and 4 display the entry potential data and mitigation system location plotted on floor plans for each of the houses. Table 5 contains descriptions of the symbols used in these figures. Because the highest radon entry potentials generally occur at the slab perimeter, SSD systems were designed to depressurize the sub-floor areas with the highest entry potentials by penetrating the exterior stem walls from outdoors. With this approach, interior locations for pipes were avoided. By penetrating the stem wall, pressure fields were often more easily extended along the perimeter through the existing gaps, channels, and more permeable materials. As seen in Table 6, the installations based on control of local areas with high radon entry potentials have been very successful in houses AL04, SF31, and TI42. Of these three houses, the SSD pressure field extends through a relatively permeable layer of soil beneath the entire slab only in SF31.

Table 5. Description of Symbols Used in Figures 3 and 4.

Symbol	Description
IF(1,2,3...)	Floor Test Hole Identification
(YES)/(NO)	Pressure Field Developed by SSD Mitigation System Detected at this Test Hole
R_S	Effective Resistance of Soil (R_{S-EFF}), 10^6 Pa-s/m^3
R_F	Effective Resistance of Substructure Floor (R_{F-EFF}), 10^6 Pa-s/m^3
G	Soil Gas Entry Potential, 10^{-6} m^3/Pa-s
RN	Soil Gas Radon Concentration, pCi/L
E	Radon Entry Potential, 10^{-3} Bq/Pa-s
VAC. HOLE	Location of Pressure Field Extension Test Using Vacuum Cleaner
SSD PIPE or SYSTEM	Subsurface Depressurization System for Radon Control

(a) AL02

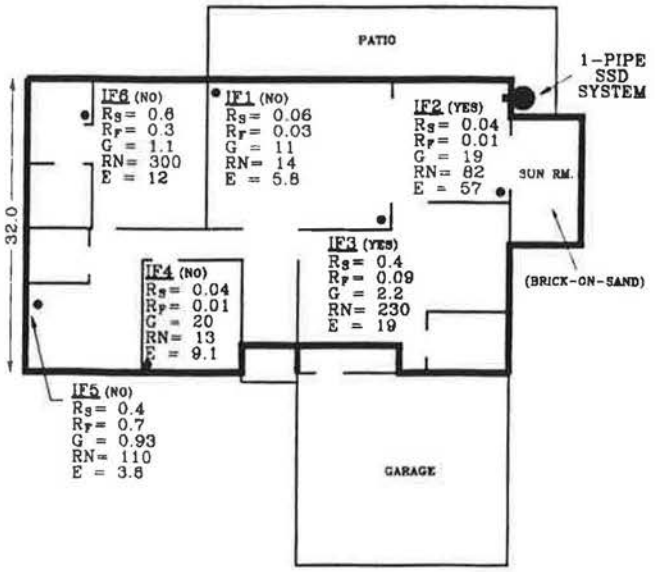

(b) AL03

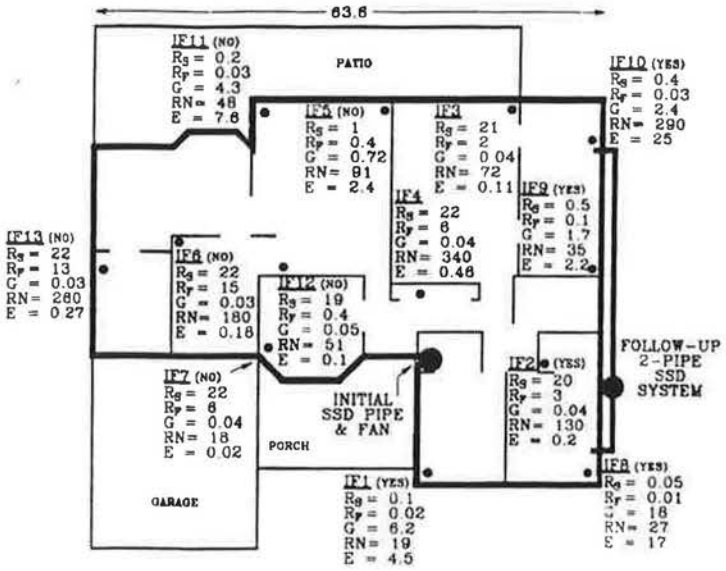

(c) AL04

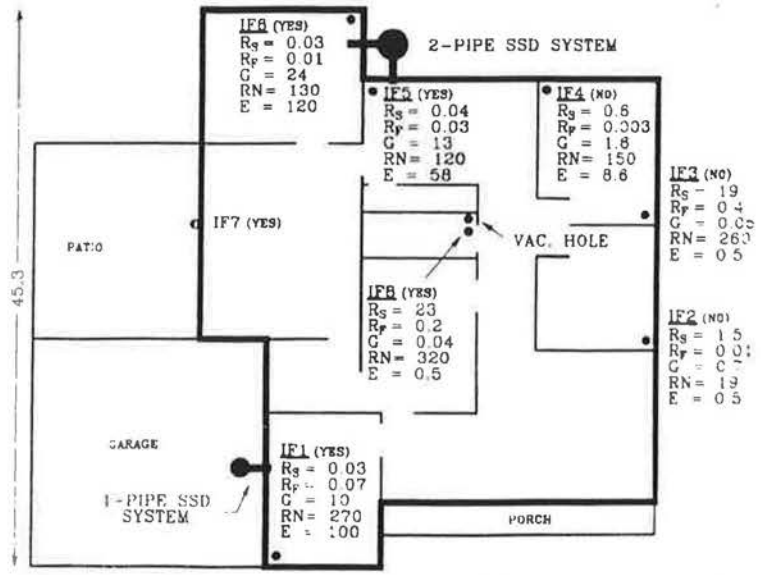

Figure 5a,b,c. Site plans of houses AL02, AL03, and AL04 show entry potential data and location of mitigation systems. The scale (in feet) for each house is shown in the dimension line. Table 5 contains descriptions of the symbols.

(a) SF31

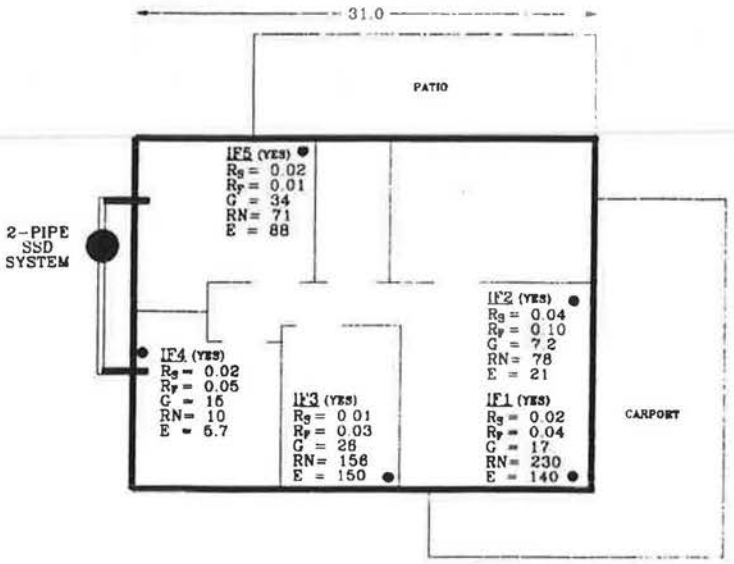

(b) TI41

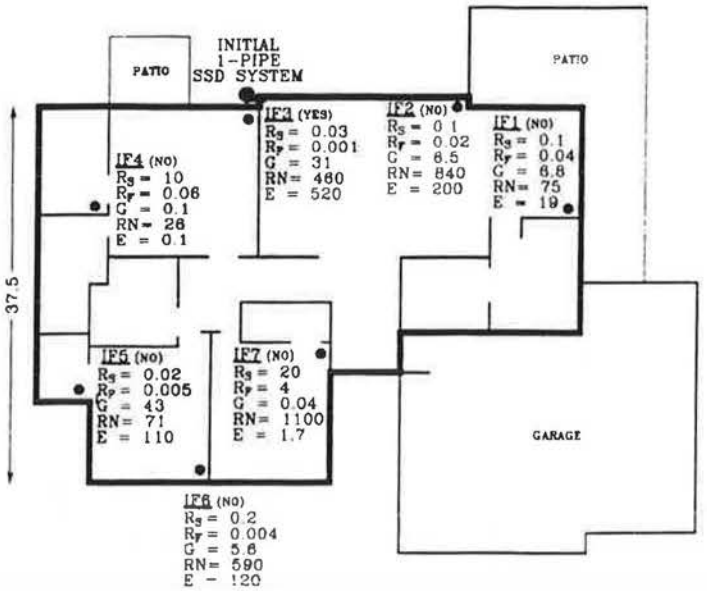

(c) TI42

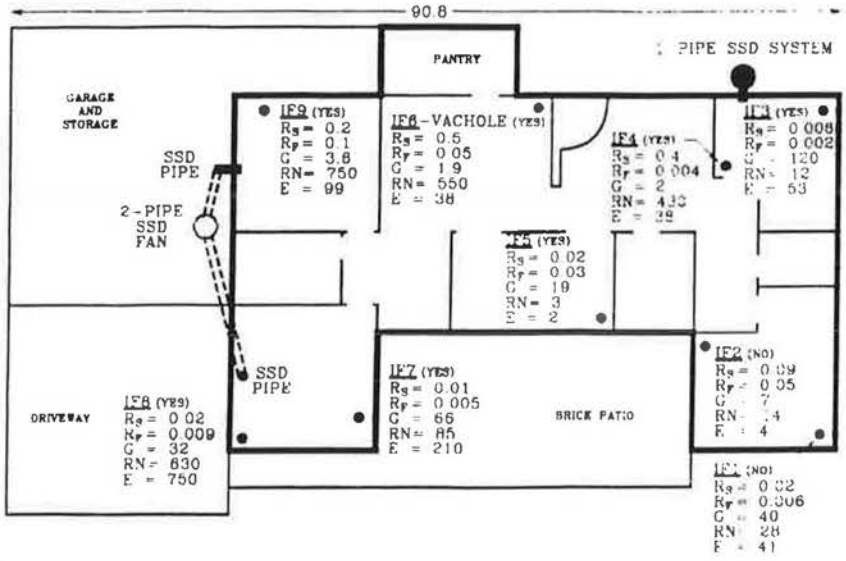

Figure 4a,b,c. Similar to Figure 3, except for houses SF31, TI41, and TI42.

There are various reasons for the lower effectiveness of the mitigation systems in the other three houses. The single SSD pipe installed in TI41 has reduced indoor radon levels approximately 40%, but is not extending the pressure field to other important radon entry locations (IF2, IF5, and IF6). Since SSD mitigation systems are being evaluated before any cracks and holes are sealed, the large perimeter crack in this house has not been sealed. During future mitigation, this crack will be sealed to improve the extension of the pressure field and additional SSD pipes will be installed, if necessary. Both AL02 and AL03 are unique in that their indoor radon levels are very responsive to changes in barometric pressure. A negative rate of change (drop) in barometric pressure appears to cause an increase in indoor radon levels, while a positive rate of change (rise) in barometric pressure causes radon levels to decrease. From the perspective of this study, two questions are raised by this condition: a) what is the mechanism forcing radon into the houses, and are existing mitigation techniques appropriate, and b) should diagnostic (entry potential) measurements and post-mitigation radon monitoring be conducted only during periods of falling barometric pressure? In house AL02, indoor radon levels appear to have been reduced approximately 70% to an average of about 80 Bq/m³. However, indoor radon levels have peaked over 520 Bq/m³ during periods of falling barometric pressure with the SSD system operating. A similar, though more difficult, problem exists at AL03 where two SSD systems have been installed that are only partially effective.

Although soil gas entry rates may be low at the center of slabs, in areas of the country where soils have extremely high radon concentrations, radon entry potentials in the center of the slabs could be quite high. In these situations, radon control may have to extend to all locations of the slab.

Table 6. Entry Potential Data and Pre- and Post-Mitigation Indoor Radon Levels - New Mexico Houses

	Soil Gas Entry Potential (E) at 10 Pa			Radon Entry Potential (E) at 10 Pa		Pre-Mitigation (after 11/1/90)		Post-Mitigation (after 11/1/90)	
House ID	Geo. Mean (10^{-3} m³/Pa-s)	Geo. Std. Dev.	Number Loc.	Geo. Mean (10^{-7} Bq/Pa-s)	Geo. Std. Dev.	Mean Indoor Rn (Bq/m³)	Approx. Duration (hrs)	Mean Indoor Rn (Bq/m³)	Approx. Duration (hrs)
AL02	4.6	4.10	6	12	2.62	290	1250	80	560
AL03	1.20	11.6	13	0.83	8.98	260	1110	140/150*	470/290*
AL04	1.30	14.2	7	6.8	13.6	290	840	40	440
SF11	[illegible]	1.80	5	47	4.14	360	1040	50	400
TI41	[illegible]	14.9	7	24	21.7	440	1540	250	150
TI42	[illegible]	3.68	9	42	6.10	590	1070	40	120

* Two different SSD mitigation systems were evaluated.

SUMMARY

Data on soil gas and radon entry potentials from this study of New Mexico houses with slab-on-grade substructures support the results from an earlier study of New Jersey houses with basements. Soils and materials surrounding the substructures of the houses in both studies are many times more resistant to soil gas flow than the below-grade structure surfaces and materials. Those areas of the substructure closer to the open soil surface tended to have higher soil gas entry potentials. Locations away from the perimeter of the slab floors in the New Mexico houses generally also had much lower radon entry potentials. Radon mitigation designs incorporating this information emphasized that pipes for SSD systems in these houses should be located along the perimeter of the slab and only at areas of relatively high radon entry potentials. Some difficulties with this diagnostic approach have been encountered in two houses where indoor radon levels are very responsive to changes in barometric pressure. Radon entry potentials were modestly correlated with average indoor radon levels during the heating season, implying that with additional modifications to the technique and analysis, radon entry potentials might be a satisfactory indicator of long-term indoor radon levels.

ACKNOWLEDGEMENTS

The authors would like to acknowledge the assistance of John Hawley of the New Mexico Bureau of Mines and Mineral Resources for his interpretation of the soils and geology at each house site, Gregory Powell for his work on the radon control systems, and all homeowners for their active participation in this project.

This work is supported by the U.S. Environmental Protection Agency (EPA) AEERL through the New Mexico Institute of Mining and Technology, Cooperative Agreement No. CR-816688-01-0. This paper has been reviewed in accordance with the U.S. EPA's peer and administrative review policies and approved for presentation and publication.

REFERENCES

1. Turk, B.H., Harrison, J., Prill, R.J., and Sextro, R.G. Developing soil gas and ^{222}Rn entry potentials for substructure surfaces and assessing ^{222}Rn control diagnostic techniques. Health Physics. 59: 405-419, 1990.

2. Nazaroff, W.W., and Sextro, R.G. Technique for measuring the indoor ^{222}Rn potential. Environmental Science and Technology. 23: 451, 1989.

3. Schery, S.D. The design of accumulators and their use in determin-

ing the radon availability of soil. In: Proceedings of the 82nd Annual Meeting of the Air and Waste Management Association. 89-79.2, Anaheim, CA, 1989.

4. Sextro, R.G., Nazaroff, W.W., and Turk, B.H. Spatial and temporal variation in factors governing the radon source potential of soil. In: Proceedings: The 1988 Symposium on Radon and Radon Reduction Technology, Volume 1, EPA-600/9-89/006a (NTIS PB89-167480). pp. 5-61 to 5-74. Research Triangle Park, NC, 1989.

5. Nazaroff, W.W., Lewis, S.R., Doyle, S.M., Moed, B.A., and Nero, A.V. Experiments on pollutant transport from soil into residential basements by pressure-driven airflow. Environmental Science and Technology. 21: 459, 1987.

6. Sextro, R.G., Moed, B.A., Nazaroff, W.W., Revzan, K.L., and Nero, A.V. Investigations of soil as a source of indoor radon. Chapter 2. In: P.K. Hopke (ed.), ACS Symposium Series No. 331, Radon and Its Decay Products: Occurrence, Properties, and Health Effects. pp. 10-29. American Chemical Society, New York, NY, 1987.

7. Mowris, R.J., and Fisk, W.J. Modeling the effects of exhaust ventilation on ^{222}Rn entry rates and indoor ^{222}Rn concentrations. Health Physics, 54: 491-501, 1988.

8. Scott, A.G., and Findlay, W.O., Demonstration of remedial techniques against radon in houses on Florida phosphate lands. EPA-520/5-83-009 (NTIS PB84-156157). Montgomery, AL, 1983.

9. Personal communication with Claus Andersen, Lawrence Berkeley Laboratory and Riso National Laboratory, Denmark, 1990.